Electronic Supplementary Material (ESI) for Chemical Science.

Cite this: DOI: 10.1039/c0xx00000x

www.rsc.org/xxxxxx

ARTICLE TYPE

Electronic Supplementary Information (ESI)

MOF Catalysis in Perspective to their Homogeneous Counterparts and Conventional Solid Catalysts

Pilar García-García,[‡,a] Maike Müller[‡,a] and Avelino Corma*[a]

General Remarks

Theoretical pattern were calculated using the data available either from the respective article or data received by the Cambridge Crystallographic Data Centre (CCDC) or the Crystallography Open Database (COD).

Experimental

Materials and methods.

PXRD: Powder X-Ray diffraction patterns were collected using a PANalytical CUBIX Diffractometer with CuK_α radiation ($\lambda_1 = 1.54056$ Å, $\lambda_2 = 1.54439$ Å, I2/I1 = 0.5, tube voltage 45 kV, intensity 40 mA), equipped with an X'Celerator detector, Bragg–Brentano geometry, an automatic divergence slit (2.5 mm), and a goniometer arm length of 200 mm. The scan range was 2.0° to 90.0° (2θ) with a scan step size of 0.040° (2θ) and a counting time of 34.92 s per step. *EA*: C, N and H analyses were carried out using a Carlo Erba 1106 elemental analyser. *ICP-AAS:* For the determination of the metal content (Zn) the analyses were carried out on a Varian 715-ES inductively coupled plasma-optical emission spectrometer. Prior to the measurement, the samples were dissolved in a 3:1:1 HNO_3/HCl/HF aqueous solution. *TG/DTA:* Thermogravimetric and differential thermal analyses (TGA-DTA) were carried out in N_2 stream using a Mettler Toledo TGA/SDTA 851E instrument in a temperature range of r.t. to 800°C. *FT-IR:* FTIR spectra were obtained using a Nicolet 710 spectrometer (4 cm^{-1} resolution). The samples were prepared as KBr disks and measured at room temperature. *N_2 sorption studies:* N_2-sorption studies were performed using a Micromeritics ASAP2010 Accelerated Surface Area and Porosimetry System at 77 K. the samples were outgassed prior to the measurement (120°C, 12 h). The specific surface area was calculated from the nitrogen adsorption data in a relative pressure range from 0.04 to 0.2 and the measures type I isotherm was fitted to the BET model.

Synthetic procedures.

All reagents, HKUST-1, Basolite A100 and Basolite F300 were purchased from commercial suppliers.

Synthesis of Metal organic frameworks: MIL-100 (Fe),[120] MIL-53 (Al),[121] Cu(bdc)[34], UiO-66,[28] and UiO-66-NH_2[122] and the aluminium phosphates ALPO-5, Cu-ALPO-5, Fe-ALPO-5, and Zr-AlPO-5 have been synthesized according to known literature procedures revealing metal contents of either 0.91 wt% Cu, 0.70 wt% Fe, and 0.984 wt% Zr, respectively.[71, 123] The synthesis of $Cu(OH)_x@Al_2O_3$ (2.13 wt% Cu) has been adapted from Jin et al.[39] The copper complex supported in a hybrid organic-inorganic mesoporous material (denoted along the text as $CuCl_2(diamine)_{meso}$) has been prepared according to the reported procedure.[38] The analytic data of these materials match the reported data (see supplementary).

Synthesis of Me-AlPOs: The synthesis of Me-AlPOs with Me = Cu, Fe, Zn was performed according to the procedure reported by Blasco et al.[71] Samples with different metal contents were obtained by a hydrothermal synthesis. Triethylamine was used as a template within gels with a Al_2O_3:P_2O_5:TEA:H_2O ratio of 0.8:1:1.76:47. Orthophosphoric acid (85%), pseudoboehmite (Catapal A Sasol) were used as reagents. Metals were generally introduced in the synthesis gels as inorganic metal salts, e.g. $Zn(NO_3)_2$*6H_2O.

The gels were introduced in Teflon-lined stainless steel autoclave and heated in static conditions at 200 °C for more than 15 h. The samples were centrifuged at 10,000 rpm, washed with deionized water and dried at 373 °C overnight.[71]

Synthesis of Zr-AlPO-5: The synthesis of Zr-AlPO-5 was performed according to the procedure reported by Dongare *et al.*[123] with a synthesis gel of TEA:xZrO_2:Al_2O_3:P_2O_5:33H_2O. In a typical synthesis, 20.8 g of aluminium isopropoxide were stirred in 80 g of dry isopropanol at 60°C for 1 h. Then 0.66 g zirconium propoxide and 20 g isopropanol were added under vigorous stirring. The mixture is stirred for another 45 min, then warmed to 70°C to evaporate isopropanol. Afterwards, 11.5 g H_3PO4 was added together with 30 g of water. The mixture is stirred for 1h and then 7.6 g TEA was added slowly and stirring was continued for 1h. The gel was then placed in a teflon-lined stainless steel autoclave and heated at 200°C for 5 days. The resulting white solid is filtered off, washed with deionized water and dried at 100°C. Finally, the solid was calcined in air at 600°C for 8 h.

Catalysis

The percentage conversion and relative yields of reactants and products were determined using an Agilent gas chromatograph with FID detector and high purity helium as carrier gas. The products were identified by comparison with standard samples.

Alcoholysis of styrene oxide: The reaction was carried out using 0.2 mmol of catalyst in 5 ml (125 mmol) MeOH if not otherwise indicated. 2 mmol of styrene oxide are added to the suspension/solution. The reaction was carried out at 40°C for 24 h by stirring at 500 ppm. The progress of the reaction was followed by GC analysis and samples were collected continuously from the reaction mixture.

Friedel-Crafts Reaction of Pyrroles and Nitroalkenes. The corresponding catalyst (2 or 20 mol%) and trans-β-nitrostyrene (149 mg, 1.0 mmol) were placed in a round bottom flask. Dry toluene (1 mL) was added followed by methylpyrrole (133 µL, 1.5 mmol). The reaction vessel was closed tightly and the temperature was set to 100°C. The progress of the reaction was followed by GC analysis and aliquots were collected from the reaction mixture at different times. Dodecane was used as external standard.

Cyanosilylation of Aldehydes. The corresponding copper catalyst (10 mol%) was placed in a round bottom flask under N_2 atmosphere. Dried CH_2Cl_2 (1 mL or 2.5 mL) was then added followed by benzaldehyde (100 µL, 1 mmol). The temperature was set to 40°C and trimethylsilylcyanide (250 µL, 2 mmol) was subsequently added with a syringe. Aliquots were taken during the course of the reaction and analysed by GC using dodecane as external standard to follow the progress of the reaction.

Copper-Catalysed Huisgen Cycloaddition reaction between Alkynes and Azides. The copper catalyst (10 mol%) was placed in a round bottom flask connected to a reflux condenser under N_2 atmosphere. Ethanol (6 mL) was then added, and the temperature was set to 70°C. Benzyl azide (1 mmol) and phenylacetylene (1.2 mmol) were subsequently added with a syringe. Aliquots were taken during the course of the reaction and analysed by GC using dodecane as external standard to monitor the transformation.

Copper-Catalysed Aerobic Oxidative Cross-Coupling of Terminal Alkynes and Amides. The copper catalyst (5 mol%), K_2CO_3 (6.9 mg, 0.05 mmol) and 2-oxazolidinone (261 mg, 3.0 mmol) were placed in a round bottom flask. Mesitylene (10 mL) was then added followed by phenylacetylene (110 µL, 1.0 mmol). The reaction temperature was set to 100°C and the mixture was vigorously stirred 1 atm of air. The progress of the reaction was followed by GC analysis and aliquots were collected from the reaction mixture at different times. Nitrobenzene was used as external standard.

Hydrogenation of styrene: If not otherwise indicated, 0.2 mmol of the catalyst were suspended or dissolved in 2.5 ml acetonitrile. 50 µl of styrene, 40 µl of aqueous ammonia and 36 µl of hydrazine were added. The reaction was carried out for 24 h by stirring at 500 ppm at r.t.. The progress of the reaction was followed by GC analysis and samples were collected continuously from the reaction mixture.

Additional data

Alcoholysis of styrene oxide

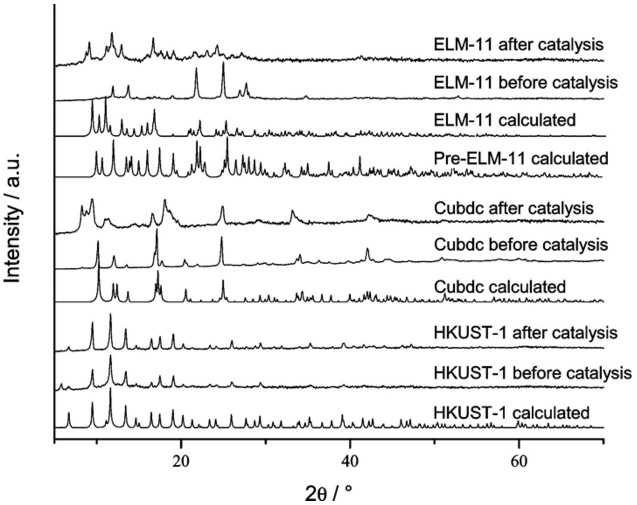

Fig. S 1 PXRD pattern of copper MOF catalysts. Pre-ELM-11, Cu(bdc) and HKUST-1 theoretical pattern are calculated from the CCDC entries 627544[124], 687690[34] and 256965[30], respectively. The theoretical pattern of ELM-11 is calculated from Kondo *et. al.* [125].

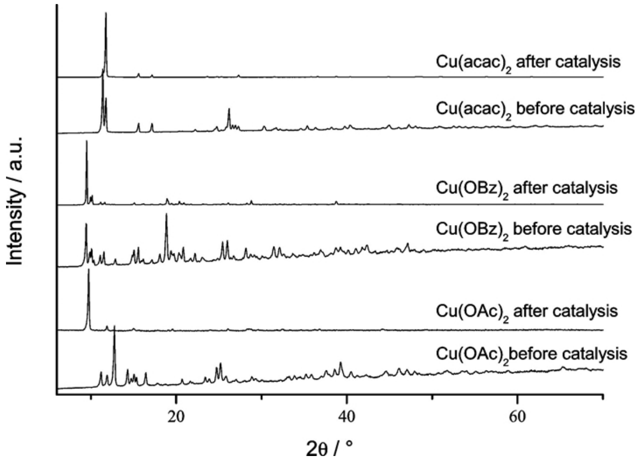

Fig. S 2 PXRD pattern of copper carboxylate catalysts.

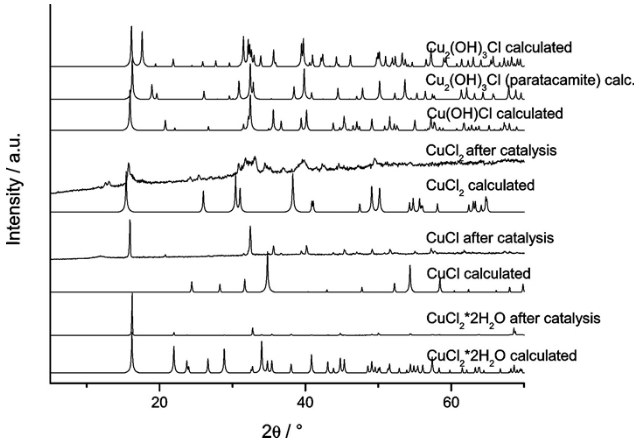

Fig. S 3 PXRD pattern of copper chloride catalysts.

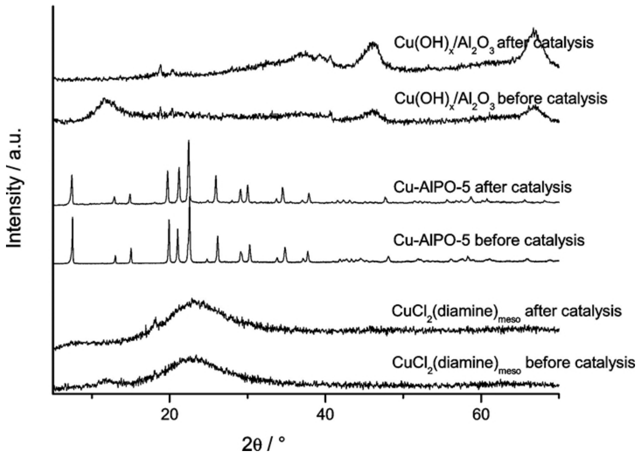

Fig. S 4 PXRD pattern of porous copper catalysts.

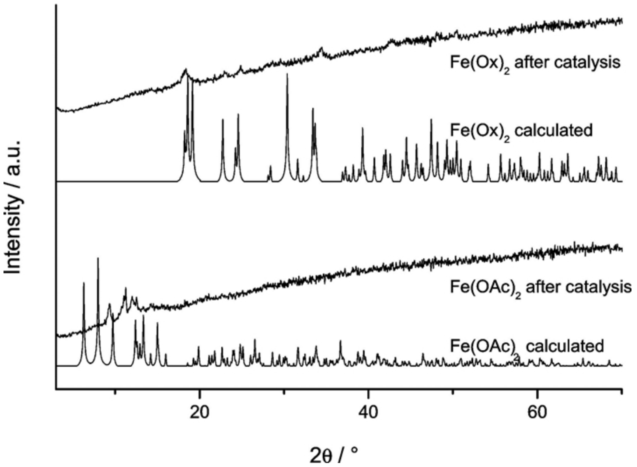

Fig. S 5 PXRD pattern of iron carboxylates. Theoretical pattern of Fe(OAc)$_2$ is calculated from the CCDC entry 747548.

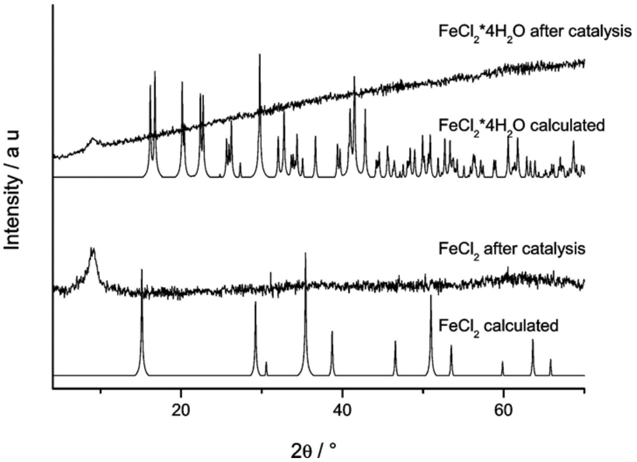

Fig. S 6 PXRD pattern of iron chlorides. Theoretical pattern of FeCl$_2$ and FeCl$_2$*2H$_2$0 are calculated from the COD entries 9009128 and XX, respectively.

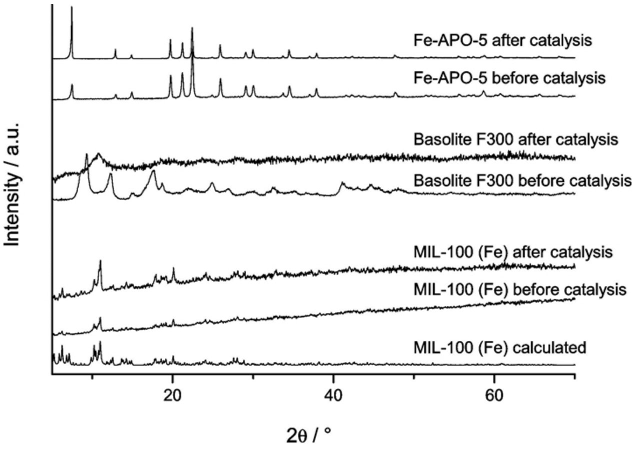

Fig. S 7 PXRD pattern of porous iron catalysts. Theoretical pattern of MIL-100 (Fe) is calculated from the CCDC entry 640536.

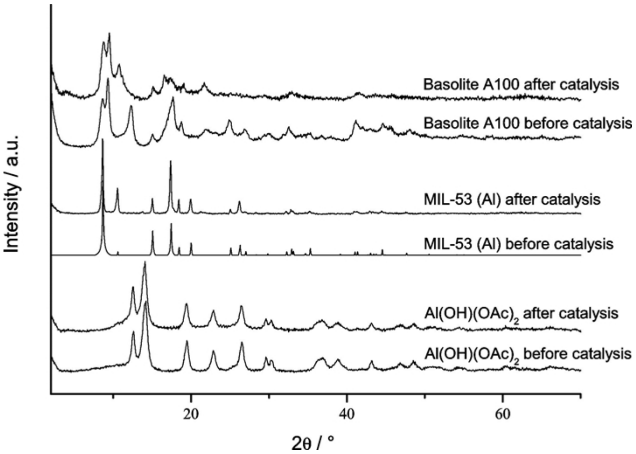

Fig. S 8 PXRD pattern of aluminium carboxylate catalysts.

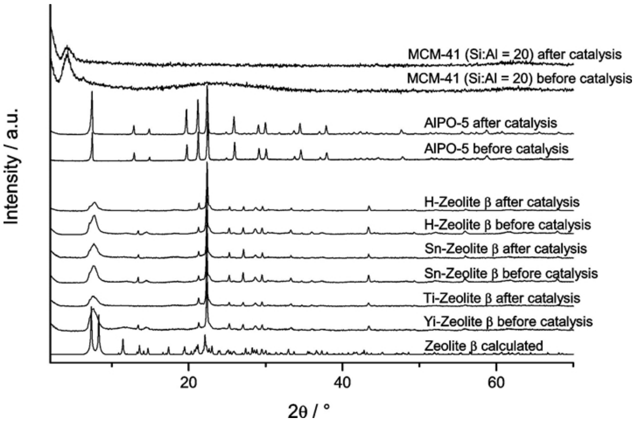

Fig. S 9 PXRD pattern of porous catalysts.

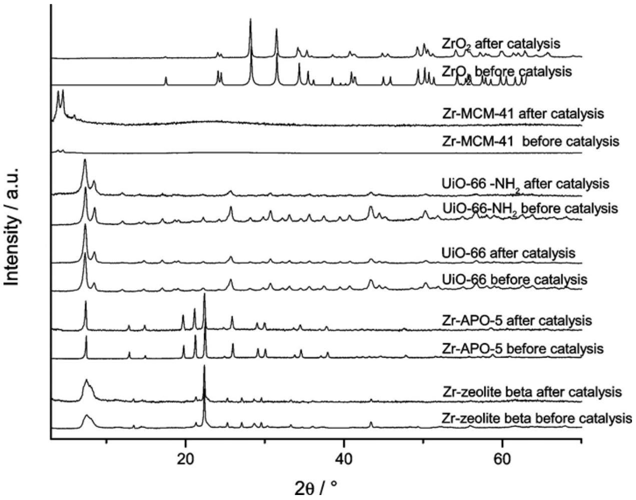

Fig. S 10 PXRD pattern of zirconium catalysts.

Hydrogenation of styrene

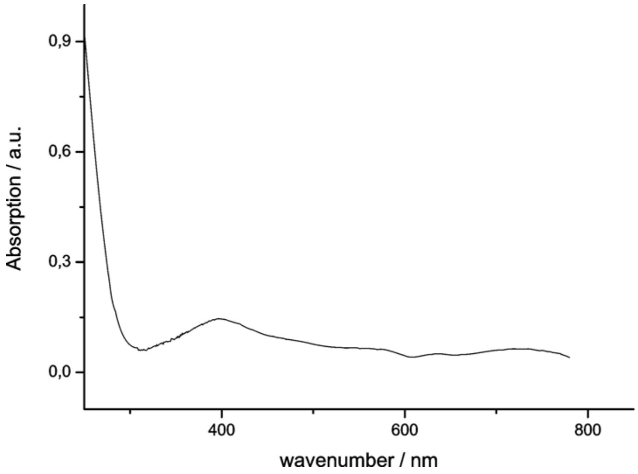

Fig. S 11 UV-Vis spectra of Cu-AlPO-5.

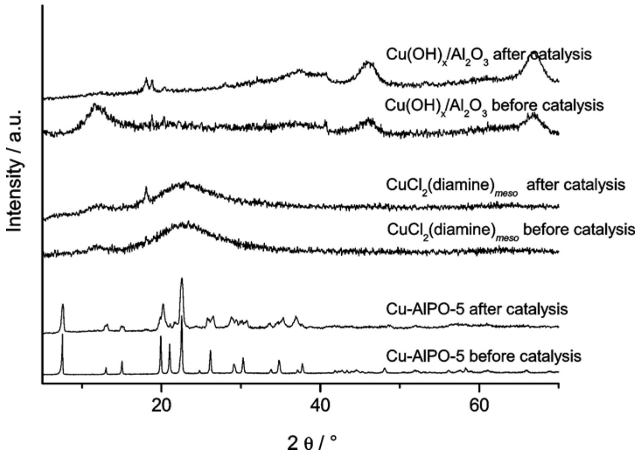

Fig. S 12 PXRD pattern of porous copper materials.

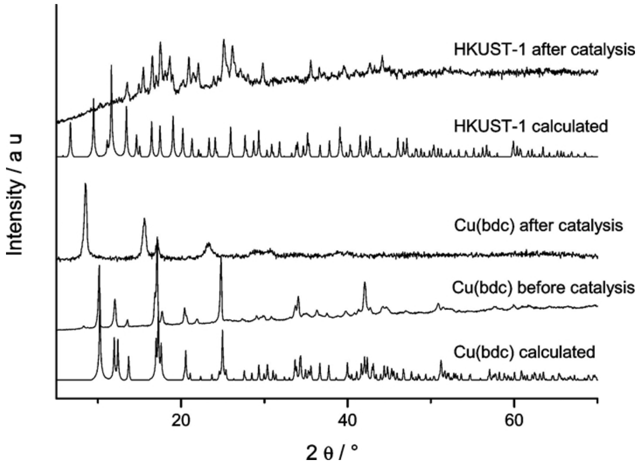

Fig. S 13 PXRD pattern of copper MOFs Cu(bdc) and HKUST-1. The theoretical pattern are calculated from the CCDC entries 687690 and 256965, respectively.

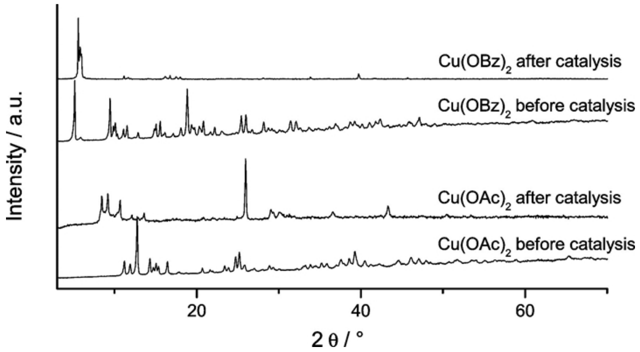

Fig. S 14 PXRD pattern of copper acetates.

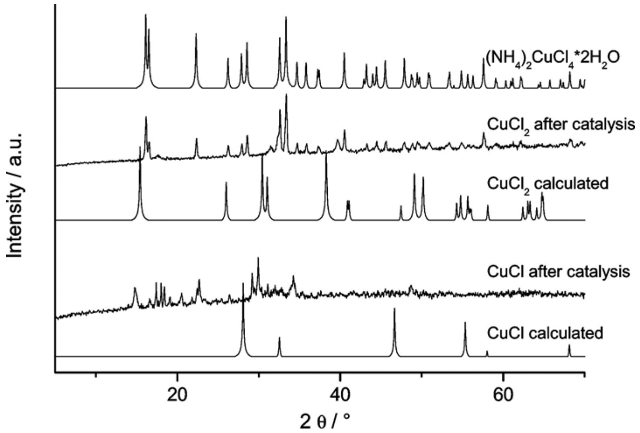

Fig. S 15 PXRD pattern of copper halides.

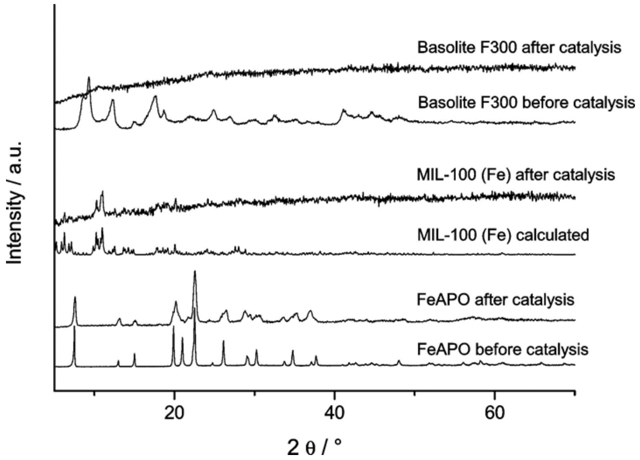

Fig. S 16 PXRD pattern of porous iron materials.

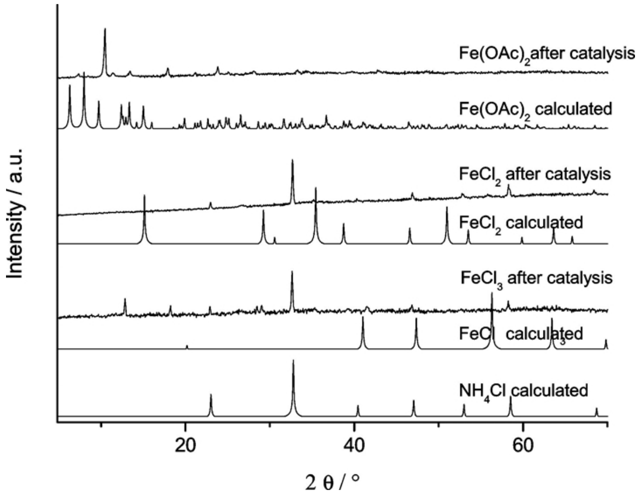

Fig. S 17 PXRD pattern of iron salts.

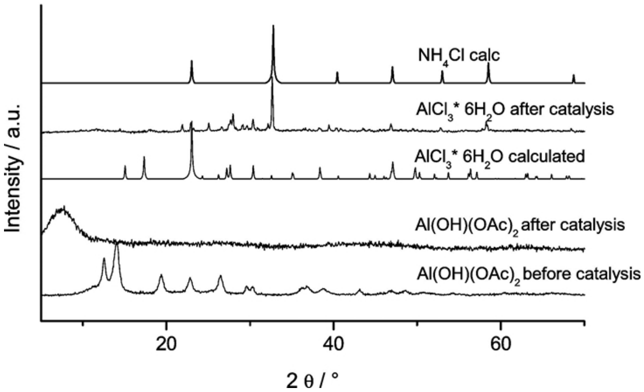

Fig. S 18 PXRD pattern of aluminium salts.

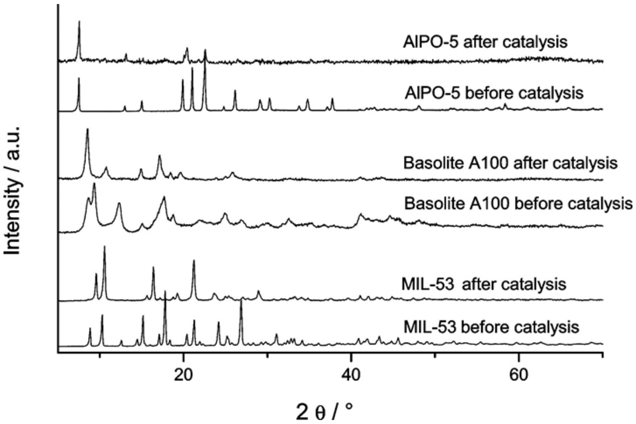

Fig. S 19 PXRD pattern of porous aluminium materials.

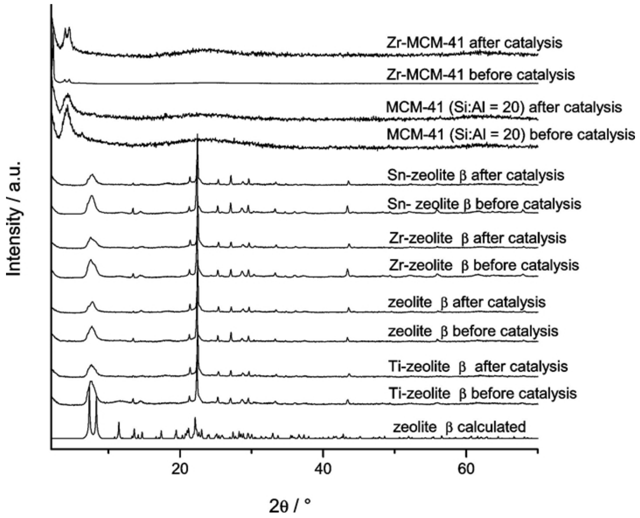

Fig. S 20 PXRD pattern of various porous materials

- Cu^{2+} salts form $Cu(NH_3)_4^{2+}$ complexes upon addition of ammonia and $CuL_x(CH_3CN)_x$ complexes/adducts in acetonitrile.
- $CuCl_2$ forms an ammine complex during the reaction, namely $(NH_4)_2CuCl_4*2H_2O$, as evidenced by the PXRD pattern.
- Fe^{III} catalyst such as $FeCl_3\cdot 6H_2O$ with the same reaction conditions might lead to the formation of a corresponding hydrazine complex, namely $FeCl_2(NH_2NH_2)_2$.[104]
- In comparison to the applied copper MOFs, the MIL-100 (Fe) framework and MIL-53 (Al) were partially stable during the reaction. The most intense Bragg reflexes at $2\theta = 4°$and 11° are observed in the PXRD pattern of the catalyst material recovered after the reaction.
- Cl containing metal salts form NH_4Cl under the reaction conditions.

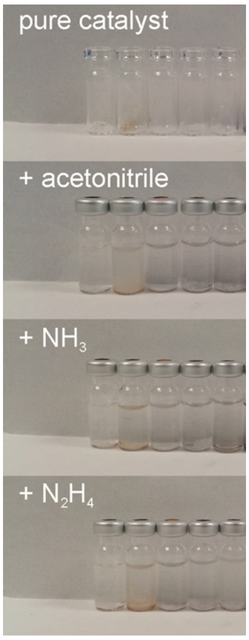

Fig. S 21 Images of various catalysts upon addition of the reactants. From left to right: AlPO-5, MIL-53 (Al), AlOH(OAc)$_2$, AlCl$_3$, Al(NO$_3$)$_3$

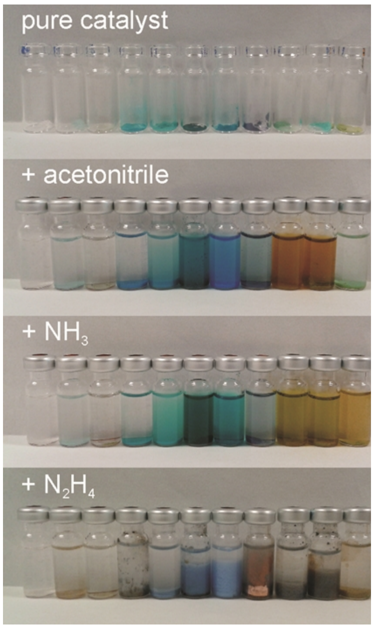

Fig. S 22 Images of various catalysts upon addition of the reactants: Cu-AlPO-5, Cu(OH)$_x$@Al$_2$O$_3$, CuCl$_2$(diamine)$_{meso}$, HKUST-1, Cu(bdc), Cu(OAc)$_2$, Cu(OBenz)$_2$ Cu(acac)$_2$ CuCl, CuCl$_2$, CuCl$_2$*2H$_2$O.

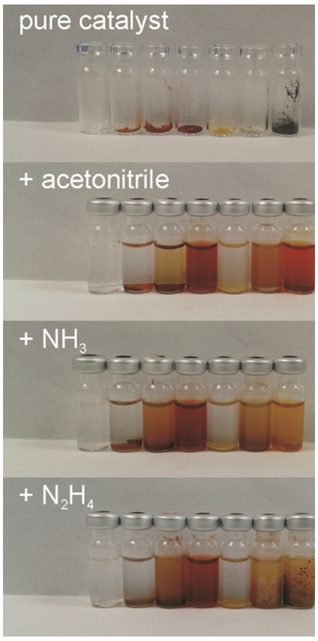

Fig. S 23 Images of various catalysts upon addition of the reactants: Fe-AlPO-5, MIL-100, $Fe(OAc)_2$, $Fe(acac)_2$, $Fe(ox)_2$, $FeCl_2*4H_2O$, $FeCl_3$